Numerical Study on the Effect of Gender on the Airflow Characteristics inside the Nasal Cavity

M Zubair [1]*, KA Ahmad [1], VN Riazuddin [1], MZ Abdullah [2], I Rushdan [3], IL Shuaib [4] and SA Khan [5]

[1]Department of Aerospace Engineering, Universiti Putra Malaysia, 43400 Serdang, Selangor, Malaysia.
[2]School of Mechanical & Aerospace Engineering, Universiti Sains Malaysia,14300 Nibong Tebal, Pulau Pinang, Malaysia.
[3]School of Medical Sciences, Health Campus, Universiti Sains Malaysia, 16150 Kubang Kerian, Kelantan, Malaysia.
[4]Advanced Medical & Dental Institute, Universiti Sains Malaysia, 13200 Kepala Batas, Pulau Pinang, Malaysia.
[5]Department of Mechanical Engineering, Higher College of Technology, Muscat, Oman.

Abstract

Understanding the properties of airflow in the nasal cavity is very important in determining the nasal physiology and in diagnosis of various anomalies associated with the nose. This numerical study presents the characteristic flow features inside a female nasal cavity in comparison with the male models developed by other researchers. The study is based on the numerical model obtained from computed tomographic data of a healthy Malaysian subject. A steady state Reynold Averaged Navier-Stokes and continuity equations was solved for both inspiratory and expiratory phase with flow rates of 7.5, 10 and 15 L/min for laminar case and 20, 30 and 40 L/min studies were simulated for turbulent boundary conditions. The differences observed in the flow parameters can be attributed to the anatomical variations that exist between the male and female nasal cavity. It was found that the female models were slightly smaller in length when compared to the male models. The nasal valve region was located about 2.0 cm, 1.65 cm and 2.5 cm from the anterior tip of nose. The value of maximum velocity obtained for the three female models are 3.17, 2.68, and 2.23 m/s respectively as against 4.2 m/s for similar flow rate obtained for the male model. The values of pressure drop for female cases were lower than the male models in the literature. In general, the female model displayed lower values of pressure drop when compared with the male models.

***Corresponding email**: E-mail: mdzubairmanipal@gmail.com (M. Zubair)

1. Introduction

Several researchers have shown the benefits of computational fluid dynamics (CFD) in better understanding of flow through the nasal cavity (Wen et al., 2008; Mylavarapu et al., 2009; Segal et al., 2008; Weinhold et al., 2004; Zubair et al., 2013a; Zubair et al., 2013b). However, most of the researchers employed male human subject in the determination of the nasal patency. Differences in inter-human anatomy and physiological morphology are observed based on gender. No specific numerical modeling studies have been carried out to compare and ascertain the effect of gender on the flow features inside the nasal cavity. Gender differences are an important determinant of clinical manifestations of airway diseases. Rowley et al. (2002) observed that though obstructive sleep apnoea was prevalent in both the gender, its effect on male subjects could be prominently observed. Using upper airway imaging, they measured upper airway cross-sectional area and retro palatal compliance in wakefulness and non-rapid eye movement (NREM) sleep in 15 men and 15 women without sleep-disordered breathing. Cross-sectional area at the beginning of inspiration tended to be larger in men compared with women in both wakefulness (194.5 $\pm$ 21.3 vs. 138.8 $\pm$12.0 (SE) mm^2) and NREM sleep (111.1 $\pm$ 17.6 vs. 83.3 $\pm$11.9 mm^2; P = 0.058). The retro palatal compliance was also observed to be higher in men during both wakefulness (5.9 $\pm$ 1.4 vs. 3.1 $\pm$ 1.4 mm^2 / cmH$_2$O; P = 0.006) and NREM sleep (12.6 $\pm$ 2.7 vs. 4.7 $\pm$ 2.6 mm^2 / cmH$_2$O; P =0.055).

Brooks et al. (1992) reported normal pharyngeal areas of 3.63$\pm$0.10 and 3.20 $\pm$ 0.09 cm^2 in western men and women, respectively. A related study by Huang et al. (1998) who addressed the gender-based differences taking into account 181 Japanese subjects, found significant differences in male and their female counterparts. Pharyngeal collapse was more predominant among males than in females; the pharyngeal compliance values were 0.104$\pm$0.007 for elderly male subjects, and 0.060$\pm$0.009 cm^2/cmH$_2$o for elderly females. Also there is a higher prevalence of irregular breathing phenomenon among men when compared to women during sleeping, and also men have larger upper airways in sitting and supine positions (Thurnheer et al., 2001). Thus the importance of studying the effect of gender on breathing phenomenon is obvious. All the previous numerical studies on nasal airflow have generalized the behavior to both the gender. A recent review by Zubair et al. (2012) has highlighted the need for carrying out gender based CFD study to evaluate the airflow behavior inside the nasal cavity.

Thus, in this study the flow phenomena inside a female nasal cavity through numerical methods for a steady state flow are presented. Studies are carried out for various flow rates of 7.5L/min, 10L/min, 15L/min, 20L/min, 30L/min and 40L/min suggesting various breathing rates. A comparative study is made of the female nasal cavity flow characteristic with that of the male nasal cavity as determined by other researchers (Wen et al., 2008; Weinhold et al., 2004; Croce et al., 2006; Cheng et al., 1996). This study of gender can be considered as the first step towards standardisation of modelling practise with respect to the nasal flow studies.

2. Methods

2.1.1 *3D model generation and meshing*

Anatomical models of the normal nasal airway were obtained from the CT scans of healthy Malaysian females. The CT scan images consisting of axial, coronal and sagittal plane were sourced from Universiti Sains Malaysia Medical Campus Hospital. The scan images were segmented slice by slice with an appropriate threshold value using the MIMICs tool (Figure 1). A correct threshold value is very important in capturing

the vital features of the nasal cavity. Hence the presence of an expert ENT practitioner is essential in deciding the threshold and editing of the geometry.
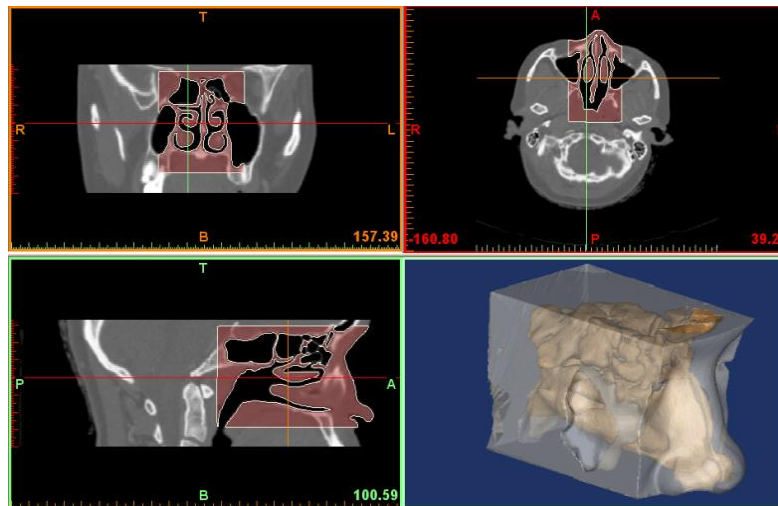

Figure 1. CT scan images from axial coronal and sagittal plane and 3D model of the human nasal cavity.

The 3D nasal cavity polylines from MIMICs was then processed using CATIA and meshed with unstructured tetrahedral elements in GAMBIT. Grid independence study was carried out using the developed 3D human nasal model. An initial coarse mesh which was obtained from GAMBIT was used to solve the airflow field at a flow rate of 7.5L/min. The original model was refined by applying gradient adaptation techniques for velocity variable. This process was repeated, with each repeat producing a model with a higher cell count than the previous model. Further adaptation was carried out for turbulent flow rates (≥20L/min) to obtain y+ value less than 5.

Figure 2 shows the grid independency study for one of the female models under consideration. When the variation in the average velocity for subsequent mesh was negligibly small, the mesh was utilized for further simulation. As can be seen in Figure 2, the variation in the average velocity at nasal valve region for female model 2 was very small beyond 400000 elements. Similar observation was recorded for rest of the models. Hence for the model 1, the mesh obtained was having 591878 elements. Similarly for model 2 and 3, the size for the mesh obtained was around 474859 and 689777 respectively. Near wall model approach was applied, where the mesh close to the wall was refined in order to resolve the near wall flow for turbulent airflow.
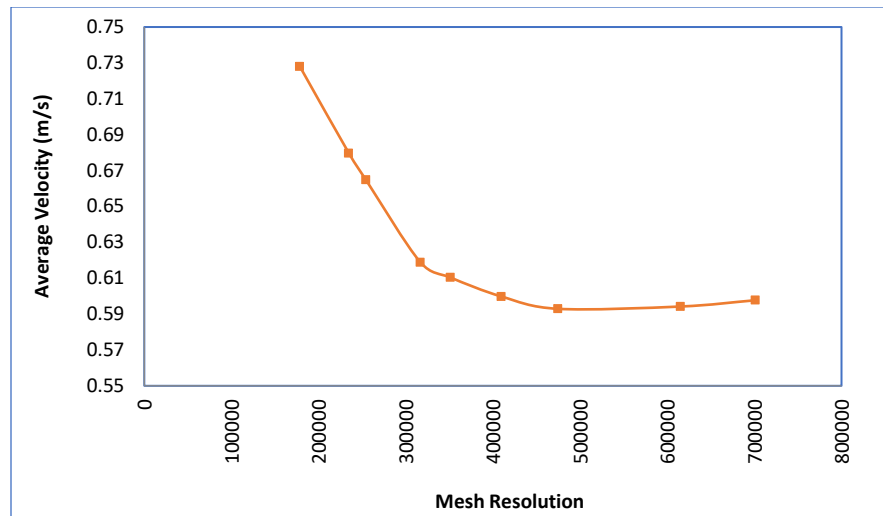
Figure 2: A sample Grid Independency study for female model 2.

2.2   Numerical model

The numerical simulation was performed using the commercial CFD solver FLUENT™. The simulation was based on the numerical solution of the Reynolds Averaged Navier-Stokes equation representing the general equation for 3D flow of incompressible and viscous fluids. The SST k-ω turbulence model, a two equation turbulence model was employed. The SST k-ω model accounts for transport of turbulent shear stress and gives highly accurate predictions of the amount of flow separation under adverse pressure gradient. The SST model is a blend of the k-ω turbulence model, which is applicable near the walls, and the k-ε turbulence model which is applied at the core of the computational domain, with an additional limiter in the formulation of the eddy viscosity to provide proper account of the turbulent SST. Therefore SST combines the advantages of both the k-ε and k-ω methods. Moreover, the suitability of SST k- ω model has been experimentally validated by Mylavarapu et al. (2009), Ahmad et al. (2010), Riazuddin et al. (2011) and Zubair et al. (2010).

The conservation and momentum equations for incompressible flow can be defined as:

$$\nabla. U = 0 \tag{1}$$

$$\rho \frac{\partial U}{\partial t} + \rho (U. \nabla) U = -\nabla P + \mu \nabla^2 U \tag{2}$$

where U is the velocity vector; P the fluid pressure and μ is the dynamic viscosity. In our simulation we adopted ρ=1.20 kg/m3 and μ=1.9 x 10-5 kg/ms.

2.3   Boundary conditions

The nasal wall was assumed to be rigid and the simulation ignored the presence of mucus. A no-slip boundary condition was defined and a plug flow with mass flow rate boundary was imposed at the nostril inlet. At the outlet, outflow boundary condition was used. Inspiration steady state laminar and turbulent airflow simulations were modeled. The airflow was assumed to be laminar for flow rates up to 15L/min the flow beyond 15L/min were turbulent. This was also in general agreement with previous researchers (Wen et al., 2008; Segal et al., 2008) who determined laminar nature of the flow, for flow less than 15 L/min. Turbulence intensity of 5% was selected for this simulation.

3.   Results and discussion

3.1   Geometry comparison

In order to verify the anatomical differences based on gender, the length of the nasal cavity was measured from a sample of available CT images. As a result a sample of 4 cases each of male and female CT nasal images were measured. Table 1 shows the total length of the nasal cavity obtained from the CT scan images of four male and four female human subjects. It was found that the female models were slightly smaller in length when compared to the male models. Based on the results shown in Table 1, we can conclude that female have shorter length of nasal cavity when compared to their male counterparts. However, this is just sample evidence which need to be further corroborated with much higher samples to verify the observations reported in Table 1. The current work is focussed on computational study of nasal cavity; hence in order to further understand the effect of gender based anatomical differences on the flow behaviour, numerical analysis has been carried out. Most of the previous works on numerical study of nasal cavity were on male models. Hence in the present work, three female healthy case models were developed from the CT images.

Table 1: The total length of the nasal cavity based on the gender comparison

Name	Length (mm)
Female 1	85.72
Female 2	89.78
Female 3	88.90
Female 4	90.97
Male 1	96.69
Male 2	91.73
Male 3	98.48
Male 4	97.37

The present female computational model was compared with the male nasal cavities from the available literature. Ten cross-sectional areas were created and used to calculate the flow properties as shown in

Figure 3. The nasal cavity extends from anterior to posterior region along the axial length. The anterior region of the nasal cavity is (x ≤ 3cm) and the posterior region (x > 5cm).

Figure 4 shows the cross-section area obtained based on the planes created across the nasal cavity. The female computational models are compared with the available male nasal cavity models. As seen in Figure 4, the total length of the nasal cavity for female subjects is shorter compared to the male model developed by Cheng et al. (1996) and Wen et al. (2008). The location of the nasal valve region also varied for each nasal model. Irrespective of gender this difference in location has also been reported by previous researchers like Keyhani et al. (1995), Subramanium et al. (1998), and Cheng et al. (1996). It can also be observed that the cross section area at the turbinate region for the female nasal cavity was wider compared to male. At the posterior region of the nasal airway, a substantial increase in cross section area was observed after the turbinate region for male. Conversely, the cross section area of the female nasal airway decreased drastically after the turbinate region. Thus it was observed that the female possessed smaller cross section area at nasopharynx.
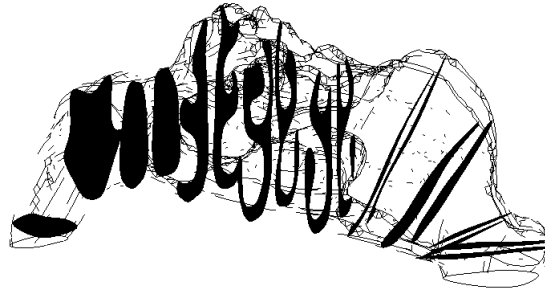

Figure 3: Location of the ten cross-sections along the axial length.
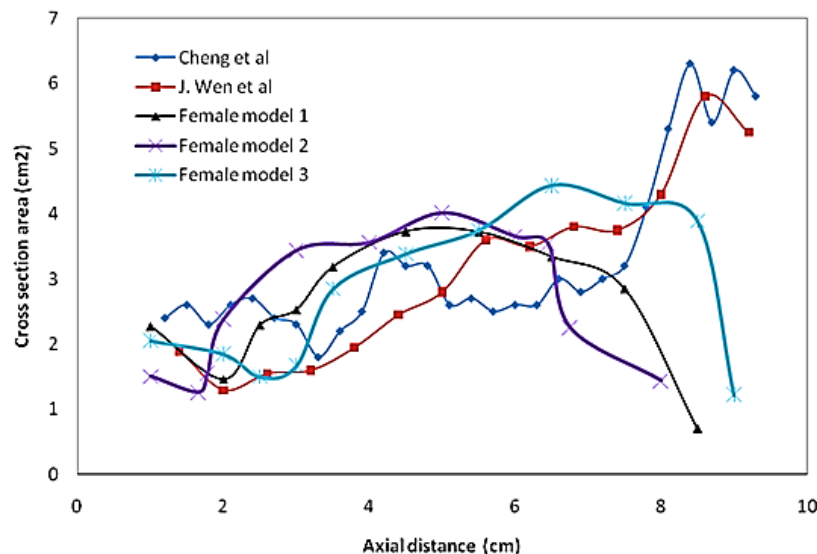

Figure 4: The comparison of cross-sectional area vs. axial distance from anterior to the posterior of the nasal cavity.

Table 2 depicts the gender-based observation for the three female models developed. Four male nasal cavity models from previous publications were considered in the current study on the basis of data available in the literature. Most of the researchers used male subjects to determine the nasal patency (Wen et al., 2008; Weinhold et al., 2004; Cheng et al., 1996; Subramaniam et al., 1998). As seen in Table 2, the female model has shorter length of nasal cavity (8.5 cm, 8 cm and 9 cm) when compared with that of the male subjects as determined by Cheng et al., 1996 and Wen et al., 2008 to be 9.3cm and 9.2cm respectively. Also, another important observation was the decrease in the cross-sectional area of the female subject when compared to male in the posterior region. The nasopharynx cross section area obtained for this study was 2.85 cm^2, 3.52 cm^2 and 2.96 cm^2, while 5.25 cm^2 and 5.8 cm^2 were determined by Wen et al. (2008) and Cheng et al. (1996) respectively. This clearly indicated that the male nasal cavity had larger posterior cross-sectional area, emphasising the variation based on gender.

Table 2: Characteristic description of nasal cavity for male and female nasal cavity models

Particulars	Male	Female
Total length of the nasal cavity	9.2 cm (Wen et al., 2008) 9.3 cm (Cheng et al., 1996)	8.5 cm (Model 1) 8.0 cm (Model 2) 9.0 cm (Model 3)
Nasapharynx cross sectional area	5.25 cm^2 (Wen et al., 2008) 5.8 cm^2 (Cheng et al., 1996)	2.85 cm^2 (Model 1) 3.52 cm^2 (Model 2) 2.96 cm^2 (Model 3)
The location of the nasal valve region	3.3 cm (Cheng et al., 1996) 2.0 cm (Wen et al., 2008)	2.0 cm (Model 1) 1.65 cm (Model 2) 2.0 cm (Model 3)
Nasal valve cross section area	1.4 cm^2 (Wen et al., 2008) 1.8 cm^2 (Cheng er al., 1996)	1.5 cm^2 (Model 1) 1.26 cm^2 (Model 2) 1.84 cm^2 (Model 3)
Pressure drop (for flow rate of 20L/min)	18 Pa (Wen et al., 2008) 20 Pa (Weinhold et al., 2004)	22.6 Pa (Model 1) 4.88 Pa (Model 2) 13.88Pa (Model 3)
Maximum velocity at nasal valve (for flow rate of 15L/min)	4.2 m/s (Subramaniam et al., 1998)	3.17 m/s (Model 1) 2.68 m/s (Model 2) 2.23 m/s (Model 3)

Although anatomical variation between male and the female model exists, a general trend could be observed. An increase in the cross- sectional profiles was observed after the nasal valve region. For the present female cases, the nasal valve region was located about 2.0 cm, 1.65 cm and 2.5 cm from the anterior tip of nose. In case of the other models available in literature, the location was at 3.3cm and 2.0cm as obtained by Cheng et al. (1996) and Wen et al. (2008) respectively. As stated earlier, irrespective of gender, the difference in location of the nasal valve has also been reported in previous literature (Keyhani et al., 1995; Subramanium et al., 1998; Cheng et al., 1996).

3.2 Comparison of flow behavior

One of the advantages of using CFD is accurate presentation of the physiological function associated with the nasal cavity. It presents useful quantification between the male and the female physiological function. The pressure drop at 20L/min obtained for the female nasal cavities was 22.6 Pa for model 1, 4.8 Pa for model 2, and 13.88 Pa for model 3 when compared with male models at around 18 Pa & 20 Pa for the same flow rate obtained by Wen et al., 2008 and Weinhold et al., 2004 respectively. The female model 1 had the smallest cross section area at the nasopharnyx outlet hence the higher value of pressure drop was obtained in comparison to model 2 and model 3. However, in general the value of pressure drop for female case 2 and 3 is lower than the male models which also correspond to the findings from the previous literature (Thurnheer et al., 2001).

Nasal valve being the critical area of the nasal cavity, comparison between the male and female models resulted in the female models exhibiting lesser value of maximum velocity when compared with the male model developed by Subramanian et al., 1998 the value of maximum velocity obtained for the three female models are 3.17, 2.68, and 2.23 m/s respectively as against 4.2 m/s for similar flow rate obtained for the male model. This shows the relative difference between the male and the female flow behaviour.

3.3 Resistance variation

The nasal resistance in the case of female model also followed the same pattern as that of the male subject under laminar flow conditions. However for turbulent flow rates, resistance curves as seen in Figure 5 was much steeper. There are significant differences in the values of pressure drop obtained for all the 3 female models. Model 1 exhibited higher values of resistance compared to the male model. The value of resistance for female case 2 was much lesser than that of the male model and the female case 1. Also the female case 3 showed lower values of resistance than its male counterparts. These variations in values for the three processed female case studies maybe attributed to the inter-human anatomical differences that exist between humans. Secondly, the values of resistance for the female case 1 having higher values of resistance maybe due to artifacts associated with the model itself. Also the female case 1 had the smallest cross section area at the nasopharnyx outlet which may contribute to the increased resistance. In general, the female model displayed lower values of pressure drop when compared with the male models.
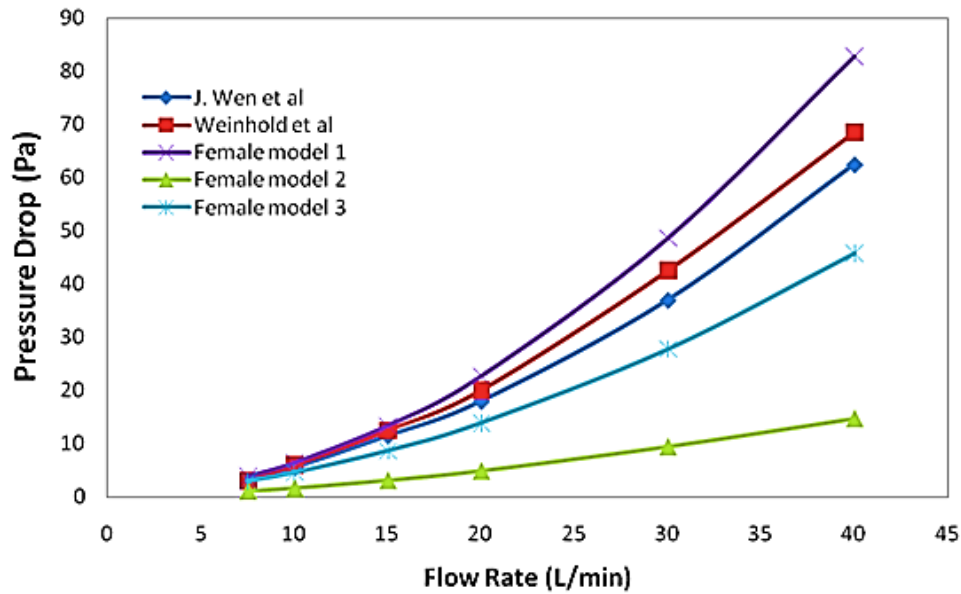
Figure 5: Pressure drop vs. inspiratory flow rates compared with previous data.

3.4 Velocity and pressure distribution

The flow was observed to be fully developed along the middle meatus region. However the superior and inferior meatus pathway received lesser flow. The peak airspeed in each plane decreased posteriorly beyond nasal valve region. These flow patterns were similar to the male models in the literature. In case of the nasal valve, which is located at the anterior region; the maximum velocity varied from 4.18 m/s , 3.57 m/s and 3.05 m/s for case 1, 2 and 3 respectively, as against 4.82 m/s & 3.1 m/s obtained by Guan-xia Xiong et al. (2008) and Croce et al. (2006) respectively. All the 3 female nasal simulations depicted similar pattern of flow behaviour inside the nasal cavity. However, due to inter-human anatomical differences, there are variations in average flow velocity as seen in Figure 6. The major deviation among the models was seen with respect to the pressure distribution in model 3 as depicted in Figure 7. Model 3 demonstrated significantly lower pressure distribution when compared to model 1 and 2 which had almost identical pressure profile. This clearly shows the difference individual anatomy has on flow patterns. Therefore, it is very difficult to standardize the results of one CFD study with other models.
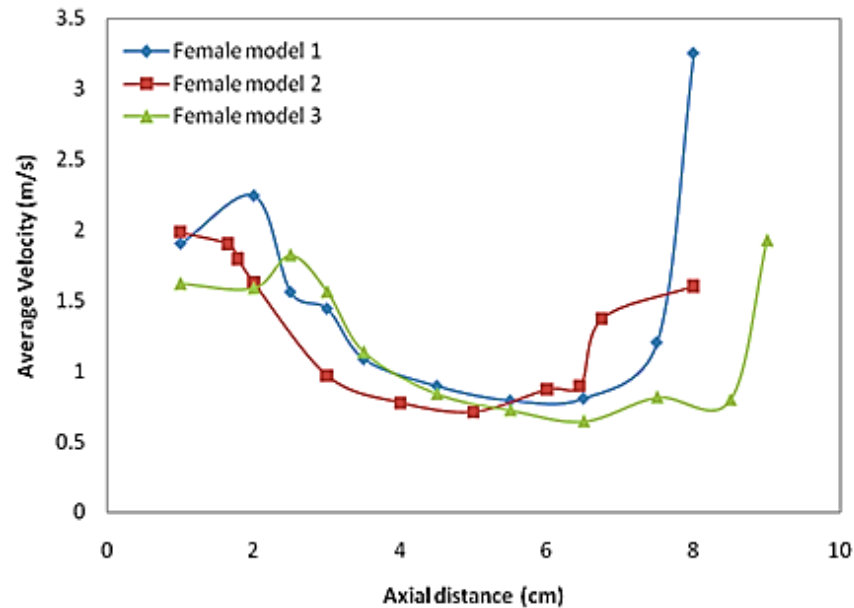
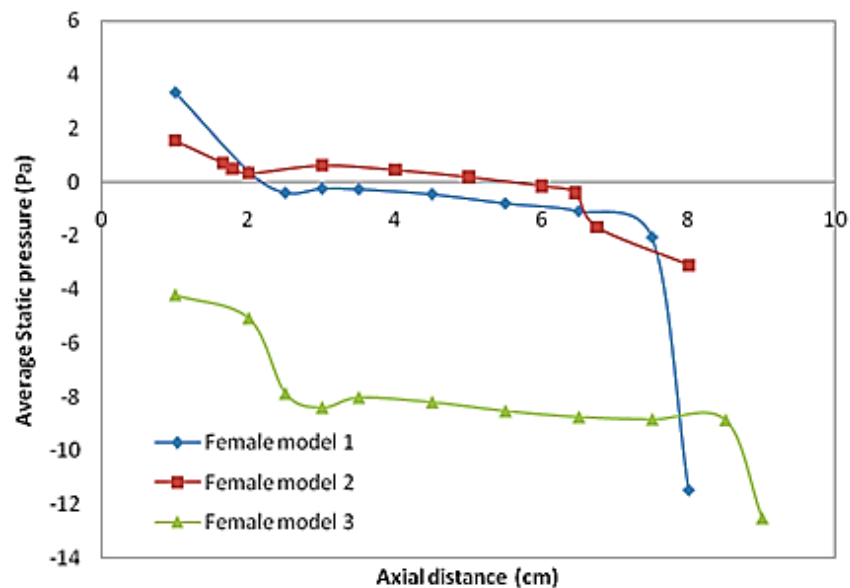Figure 6: Average Velocity across the left and the right nasal cavity

Figure 7: Static pressure vs. axial distance

3.5 Wall shear stress

Figure 8 shows the maximum wall shear stress along the axial length of the nasal cavity. The highest wall shear stress can be observed at the anterior and the posterior ends. This may be attributed to the fact that there is a sudden change in cross section at the inlet and outlet. The flow changes direction at the nasopharynx due to the bend, which results in increased value at the posterior end. At the nasal valve where there is sudden increase in velocity due to its narrow cross- sectional area, the value of the maximum wall

shear stress obtained was 0.95 Pa, 0.45 Pa and 0.42 Pa respectively. Inter-human anatomical difference does account for the difference in each of the female models depicted in Figure 9.
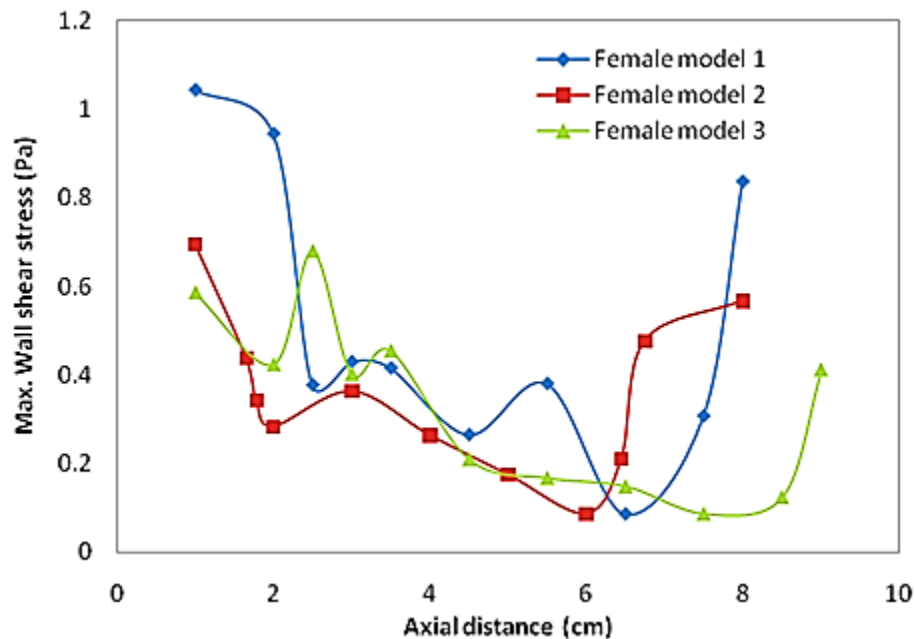

Figure 8: Maximum wall shear stress along the axial distance of the nasal cavity.

The cluster of wall shear stress developed at the nasal wall surface of female case 1 can be clearly observed as seen in Figure 9. The protruding middle turbinate in the left nasal cavity results in the high wall shear stresses. The geometry of the septum also offers resistance to flow at the wall surface and results in the increased wall shear stresses. But a predominance of the shear stresses could be observed clustered round the nasal valve region. This shows the criticality of the nasal valve during higher flow rates.
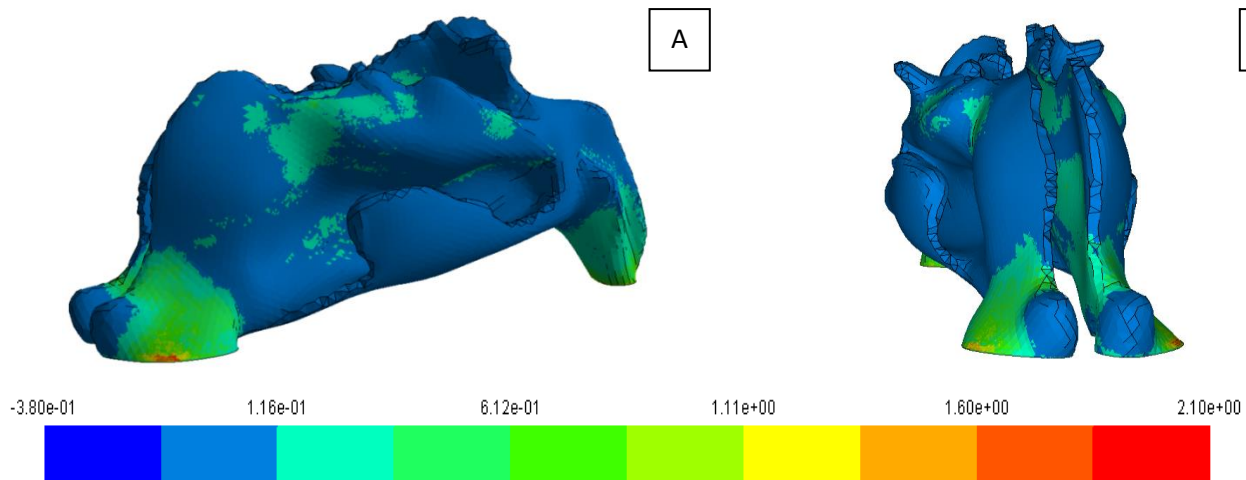

Figure 9: Wall shear stress (Pa) as indicated by a horizontal section plane in the middle region

4. Conclusions

A computational model using fluenttm was utilized to describe the nasal patency and flow through a female nasal cavity. The female model exhibited decrease in the cross sectional area at the posterior region. Also the axial length of the female nasal cavity was smaller when compared to their male counterpart. The nasopharynx cross section area obtained for female models were 2.85 cm², 3.52 cm² and 2.96 cm², as against 5.25 cm² and 5.8 cm² reported in literature for male subjects. The comparisons of the male and female nasal cavities were made indicating the importance of anatomical variations in the determination of nasal patency. The value of maximum velocity obtained for the three female models are 3.17, 2.68, and 2.23 m/s respectively as against 4.2 m/s for similar flow rate obtained for the male model. The values of pressure drop for female cases were lower than the male models in the literature. In general, the female model displayed lower values of pressure drop when compared with the male models. Thus, gender differences therefore significantly affect the flow behaviour inside the nasal cavity. Hence, we cannot generalize the result obtained from the flow simulation to either of the gender. These differences may explain the prevalence of OSA predominantly among men and not in women. Hence any future study on nasal flow should consider the effects due to gender into account.

Acknowledgements

References

Ahmad KA, Abdullah MZ, Watterson JK. (2010). Numerical modelling of a pitching airfoil. Jurnal Mekanikal; 30:37-47.

Brooks LJ, Strohl KP. (1992). Size and mechanical properties of the pharynx in healthy men and women. Am Rev Respir Dis; 146:1394–1397.

Cheng YS, Yeh HC, Guilmette RA, Simpson SQ, Cheng KH, Swift DL. (1996). Nasal deposition of ultrafine particles in human volunteers and its relationship to airway geometry. Aerosol Sci Technol; 25(3):274-291.

Croce C, Fodil R, Durand M. Sbirlea-Apiaou G, Caillibotte G, Papon JF, Blondeau JR, Coste A, Isabey D, Louis B. (2006). In vitro experiments and numerical simulations of airflow in realistic nasal airway geometry. Annals of Biomedical Engineering; 34(6):997-1007.

Huang J, Shen H, Takahashi M, Fukunaga T, Toga H, Takahashi K, Ohya N. (1998). Pharyngeal Cross-Sectional Area and Pharyngeal Compliance in Normal Males and Females, Respiration; 65:458–468.

Keyhani K, Scherer PW, Mozell MM. (1995). Numerical simulation of airflow in the human nasal cavity. J. Biomech. Eng.; 117: 429–441.

Mylavarapu G, Murugappan S, Mihaescu M, Kalra M, Khosla S, Gutmark E. (2009). Validation of computational fluid dynamics methodology used for human upper airway flow simulations. Journal of Biomechanics; 42:1553-1559.

Segal RA, Kepler GM, Kimbell JS. (2008). Effects of differences in nasal anatomy on airflow distribution: a comparison of four individuals at rest. Annals of Biomedical Engineering; 36(11):1870-1882.

Subramaniam RP, Richardson RB, Morgan KT, Kimbell JS, Guilmette RA. (1998). Computational fluid dynamics simulations of inspiratory airflow in the human nose and nasopharynx. Inhal. Toxicol.; 10: 91–120.

Riazuddin VN, Zubair M, Abdullah MZ, Ismail R, Shuaib IL, Suzina AH, Ahmad KA. (2011). Comparison of inspiratory and expiratory flow inside the nasal cavity using numerical methods. J Med Biol Eng.; 31(3):201-206.

Rowley JA, Zhou X, Vergine I, Mahdi A, Shkoukani, Badr MS. (2001). Influence of gender on upper airway mechanics: upper airway resistance and Pcrit. J Appl Physiol.; 91: 2248-2254.

Thurnheer R, Wraith PK, Douglas NJ. (2001). Influence of age and gender on upper airway resistance in NREM and REm sleep. J Appl Physiol.; 90:981-988.

Weinhold I, Mlynski G. (2004). Numerical Simulation of airflow in the human nose. Eur Arch Otorhinolaryngol.; 261:452-455.

Wen J, Inthavong K, Tu J, Wang S. (2008). Numerical simulations for detailed airflow dynamics in a human nasal cavity. Respiratory Physiology & Neurobiology; 161:125–135.

Xiong GX, Zhan JM, Jiang HY, Li JF, Rong LW, Xu G. (2008). Computational fluid dynamics simulation of airflow in the normal nasal cavity and paranasal sinuses. Am J Rhinol.; 22(5):477-82.

Zubair M, Vizy RN, Abdullah MZ, Ismail R, Shuaib IL, Suzina AH, Ahmad KA. (2010). Airflow inside the nasal cavity: visualization using computational fluid dynamics. Asian Biomed.; 4: 657-661.

Zubair M, Abdullah MZ, Ismail R, Shuaib IL, Suzina AH, Ahmad KA. (2012). A critical overview of limitations of CFD modeling in nasal airflow. J Med Biol Eng.; 32(2):77-84.

Zubair M, Abdullah MZ, Ahmad KA. (2013a). Hybrid mesh for nasal airflow studies. Comput. Math. Method Med., 2013:1-7.

Zubair M, Riazuddin VN, Abdullah MZ, Ismail R, Shuaib IL, Suzina AH, Ahmad KA. (2013b). Computational fluid dynamics study of the effect of posture on airflow characteristics inside the nasal cavity," Asian Biomed., 7: 835-840.